# J-R Curve Determination for Disk-shaped Compact Specimens Based on the Normalization Method and Direct Current Potential Drop Technique

Xiang Chen[1], Randy K. Nanstad[1], Mikhail A. Sokolov[1]

[1]Materials Science and Technology Division, Oak Ridge National Laboratory

## Abstract

Material ductile fracture toughness can be described by J-integral versus crack extension relationship (J-R curve). As a conventional J-R curve measurement method, unloading compliance (UC) becomes impractical in elevated temperature testing due to relaxation of the material and a friction induced back-up shape of the J-R curve. In addition, the UC method may underpredict the crack extension for standard disk-shaped compact (DC(T)) specimens. In order to address these issues, the normalization method and direct current potential drop (DCPD) technique were applied for determining J-R curves at 24°C and 500°C for 0.18T DC(T) specimens made from type 316L stainless steel. For comparison purpose, the UC method was also applied in 24°C tests. The normalization method was able to yield valid J-R curves in all tests. The J-R curves from the DCPD technique need adjustment to account for the potential drop induced by plastic deformation, crack blunting, etc. and after applying a newly-developed DCPD adjustment procedure, the post-adjusted DCPD J-R curves essentially matched J-R curves from the normalization method. In contrast, the UC method underpredicted the crack extension in all tests resulting in substantial deviation in the derived J-R curves manifested by high $J_q$ values than the normalization or DCPD method. Only for the tests where the UC method underpredicted the

crack extension by a very small value, J-R curves determined by the UC method were similar to those determined by the normalization or DCPD method.

## Introduction

To improve thermal efficiency, next generation nuclear reactors aim at operating at more severe environment, such as elevated temperatures and higher stress levels, than current reactors. Therefore, characterization of mechanical properties of structural materials for next generation nuclear reactors in extreme environments becomes vitally important from both engineering design and safety management point of view [1]. Among different mechanical properties of materials, J-integral verse resistance curve (J-R curve) is a useful tool for evaluating material structural integrity in the presence of pre-existing defects. Furthermore, developing material J-R curves with relatively small specimens, such as disk-shaped compact (DC(T)) specimens, gains more popularity nowadays especially in the case of post-irradiation mechanical tests because of the limitation of irradiation volume and difficulties associated with handling large irradiated specimens and their disposal [2]. To date, extensive efforts have been continuously devoted to develop simplified and reliable methods for determining material J-R curve. A widely accepted practice for conducting J-R curve testing is ASTM standard E1820-11 [3], in which the unloading compliance (UC) method is recommended for online crack length measurement. However, the UC method becomes impractical in elevated temperature testing due to stress relaxation of the material and enhanced friction interference between the specimen, pin and clevis which results in a back-up shape of the J-R curve. In addition, the UC method may underpredict the crack extension for DC(T) specimens which further limits its applications for the J-R curve determination in small specimens.

In order to address the issue associated with the J-R curve determination with the UC method, two alternative methods for deriving J-R curves, i.e. the normalization method and direct current potential drop (DCPD) technique, are investigated in this study. The normalization method was initially developed by Herrera and Landes et al. [4, 5] and later on studied by Joyce and Lee [6, 7]. In contrast to the UC method, the normalization method does not reply on the compliance measurement for on-line crack size measurement. Instead, the normalization method solely needs a load-displacement record taken together with initial and final crack size measurements from the specimen fracture surface to derive the material J-R curve. Because of the elimination of the compliance measurement, the load-displacement curve in the normalization method does not need to have the unloading-reloading portion as in the UC method (Fig. 1), which significantly simplifies the test and reduces the test time.

As another alternative J-R curve test method [8-12], the DCPD technique combines advantages of both the UC and normalization methods. It does not require the unloading compliance measurement, so the test is simplified and the load-displacement curve is same as that of the normalization method in Fig. 1. In addition, the DCPD technique provides experimental real-time crack size measurements as in the UC method. The crack size prediction in DCPD relies on the passage of a constant direct current through the specimen and the subsequent measurement of the voltage generated across an area in the specimen (Fig. 2(a)). As the crack propagates in the specimen, less area is available for the passage of the same constant current, resulting in increase of the effective electrical resistance and the potential measurement, i.e. potential drop in Fig. 2(b). Thus, a correlation exists between the crack length and potential drop in DCPD.

In this work, efforts are focusing on applying the normalization method and DCPD technique for determining J-R curves for 0.18T DC(T) specimens. Both conventional room temperature tests and elevated temperature tests are performed. For comparison purpose, the UC method is also applied to room temperature J-R curve tests.

## Experimental

### *Material and Specimens*

Standard 0.18T DC(T) specimens (Fig. 3) with W(width)/B(thickness)=2 were machined from type 316L stainless steel in both T-L and L-T orientations. Table 1 lists the material constants at two selected testing temperatures (24°C and 500°C). Each specimen was fatigue pre-cracked to $a_0$(initial crack length)/W=0.5 and then side-grooved to remove 10% of specimen thickness from each side of the specimen.

### *Test Conditions and DCPD Probe Setup*

All tests were performed with a quasi-static loading rate of 2 MPa$\sqrt{m}$/s. Two test temperatures, 24°C and 500°C, were selected, representing conventional room temperature and elevated temperature J-R curve tests. Three different J-R curve analysis methods, namely the UC method, the normalization method, and the DCPD technique, were applied in room temperature testing whereas only the normalization method and the DCPD technique were used in 500°C testing due to inherent difficulties for the UC method in elevated temperature testing.

A servo-hydraulic test frame with infrared heating was employed for fracture toughness testing. The specimen load-line displacement was measured by a clip-on displacement gage. For the DCPD measurement, current probes and potential probes were spot welded to the specimen as shown in Fig. 4. The current probes were located midway between the back end of the specimen and the center line of pin holes. Two potential probes with 0.1 inch gage span were

spot welded diagonally across the starter notch to average measurements of non-uniform crack fronts if there are any [13]. For each test, load-displacement data and DCPD signal were acquired from the same specimen simultaneously so that comparison of J-R curve results between three different analysis methods is made on the same specimen to avoid any influence due to specimen to specimen differences.

**Results and Discussion**

*J-R Curve Determination by the Normalization Method*

The procedures for applying the normalization method to the J-R curve determination can be found in Annex 15 of ASTM standard E1820-11 [3]. Specifically, procedures for applying the normalization method to DC(T) type specimens are elaborated in this section. Since the J-integral calculation in the normalization method is same as in the UC method, only the derivation of crack size in the normalization method is presented in detail.

The starting point for the normalization analysis is the specimen load verse load-line displacement record. From initial load up to, but not including the maximum load, each ith load $P_i$ is normalized using:

$$P_{Ni} = \frac{P_i}{WB(\frac{W - a_{bi}}{W})^{\eta_{pl}}} \tag{1}$$

where $\eta_{pl}$ is a dimensionless parameter that relates plastic work done on a specimen to crack growth resistance defined in terms of deformation theory J-integral [14] and equals to $2+0.522b_0/W$ here[2] and $a_{bi}$ is the blunting corrected crack size at the ith data point given by:

$$a_{bi} = a_0 + \frac{J_i}{2\sigma_Y} \tag{2}$$

[2] $b_0$ is the initial uncracked ligament and equals to $W-a_0$

where $\sigma_Y$ is the effective yield strength and equals to the average of the material yield strength and the ultimate tensile strength at the testing temperature and the provisional J-integral at the ith data point, $J_i$, is calculated from:

$$J_i = \frac{K_i^2(1-\nu^2)}{E} + J_{pli} \tag{3}$$

where $K_i$ is the stress intensity at the ith data point, ν is Poisson's ratio, E is Young's modulus of the material, and $J_{pli}$ is the plastic component of $J_i$. The equation for calculating $K_i$ is:

$$K_i = \frac{P_i}{(BB_N W)^{1/2}} \times \frac{(2+\frac{a_i}{W})[0.76+4.8(\frac{a_i}{W})-11.58(\frac{a_i}{W})^2+11.43(\frac{a_i}{W})^3-4.08(\frac{a_i}{W})^4]}{(1+\frac{a_i}{W})^{3/2}} \tag{4}$$

where $B_N$ is the net specimen thickness and $a_i$ is the crack size for the ith data point. The equation for calculating $J_{pli}$ is given by:

$$J_{pli} = [J_{pli-1} + \frac{\eta_{i-1}}{b_{i-1}} \frac{A_{pli} - A_{pli-1}}{B_N}][1-\gamma_{i-1}\frac{a_i - a_{i-1}}{b_{i-1}}] \tag{5}$$

where $\eta_{i-1}=2.0+0.522b_{i-1}/W$, $\gamma_{i-1}=1.0+0.76b_{i-1}/W$, $b_{i-1}$ is the uncracked ligament for the (i-1)th data point and equals to $W-a_{i-1}$, and $J_{pli-1}$ is the plastic part of J-integral for the (i-1)th data point and assuming $J_{pl0}$ equals to zero (initial plastic component of J-integral is zero). The quantity $A_{pli}-A_{pli-1}$ is the increment of plastic area under the load verse load-line displacement record between lines of constant plastic displacement $v_{pli}$ and $v_{pli}$-1 and can be calculated from the following equation:

$$A_{pli} - A_{pli-1} = \frac{(P_i + P_{i-1})(v_{pli} - v_{pli-1})}{2} \tag{6}$$

where $v_{pli}$, the plastic part of the ith load-line displacement data point, is given by:

$$v_{pli} = v_i - P_i C_{LLi} \tag{7}$$

where $v_i$ is the load-line displacement at the ith data point and $C_{LLi}$ is the equivalent compliance corresponding to $a_i$ and is calculated by:

$$C_{LLi} = \frac{1}{EB_e}\left(\frac{W + a_i}{W - a_i}\right)^2 \times [2.0462 + 9.6496\left(\frac{a_i}{W}\right) - 13.7346\left(\frac{a_i}{W}\right)^2 + 6.1748\left(\frac{a_i}{W}\right)^3] \quad (8)$$

where the effective thickness $B_e = B - (B - B_N)^2/B$.

Similar to each normalized load $P_{Ni}$, the load-line displacement is normalized to yield a normalized plastic displacement $v'_{pli}$ using:

$$v'_{pli} = \frac{v_{pli}}{W} = \frac{v_i - P_i C_{LLi}}{W} \quad (9)$$

where $C_{LLi}$ is given in Eq. 8.

From the first load-displacement pair up to, but not including the load-displacement pair at the maximum load, the normalized load $P_{Ni}$ and normalized plastic displacement $v'_{pli}$ given in Eq. 1 and 9 are calculated using the initial crack size $a_0$. Namely, all the $a_i$ and $a_{i-1}$ values in Eq. (4), (5), and (8) should be substituted with $a_0$. Afterwards, the last load-displacement pair is normalized using the same form in Eq. 1 and 9 but with the final crack size $a_f$:

$$P_{Nf} = \frac{P_f}{WB\left(\frac{W - a_f}{W}\right)^{\eta_{pl}}} \quad (10)$$

$$v'_{plf} = \frac{v_{plf}}{W} = \frac{v_f - P_f C_{LLf}}{W} \quad (11)$$

where $C_{LLf}$ is calculated by replacing $a_i$ with $a_f$ in Eq. 8.

All the normalized load and plastic displacement data points calculated in previous procedures are plot as in Fig. 5(a). Then a tangent line is drawn from the final data point in that plot to the remaining data as shown in Fig. 5(b). Data to the right of the tangent point will be excluded from the normalization function fit. In addition, data with normalized plastic

displacement $v'_{pli} \leq 0.001$ will also be excluded from the normalization function fit. After applying the aforementioned two eligibility criteria, qualified data are least square fitted with the following normalization function (Fig. 5(c)):

$$P_N = \frac{a + bv'_{pl} + cv'^{2}_{pl}}{d + v'_{pl}} \tag{12}$$

where a, b, c, and d are fitting constants and $P_N$ and $v'_{pl}$ represent the normalized load and plastic displacement given by the normalization function. If the normalization function can fit all the normalized load ($P_{Ni}$) and plastic displacement ($v'_{pli}$) pairs with a maximum deviation less than 1% for the final data point, the normalization method can be applied for deriving the J-R curve of the test.

Next, an iterative procedure is adopted to make $P_{Ni}$ and $v'_{pli}$ match the normalization function in Eq. 12. This involves adjusting the crack size $a_i$ used to calculate $P_{Ni}$ and $v'_{pli}$ so that the updated $P_{Ni}$ and $v'_{pli}$ would fall on the function in Eq. 12. In detail, for the first load-displacement pair with the original $v'_{pli} \geq 0.002$ and assuming $a_i = a_0$, the normalized load is recalculated as:

$$P_{Ni} = \frac{P_i}{WB\left(\frac{W - a_i}{W}\right)^{\eta_{pl}}} \tag{13}$$

and $v'_{pli}$ is recalculated as in Eq. 9. The recalculated $v'_{pli}$ is inputted as $v'_{pl}$ in Eq. 12 to calculate $P_N$. Then $P_N$ is compared with $P_{Ni}$ in Eq. 13. If the difference between $P_N$ and $P_{Ni}$ is larger than ±0.1%, the crack size $a_i$ is adjusted from $a_0$ and $P_{Ni}$ and $v'_{pli}$ is recalculated with the adjusted $a_i$. Afterwards, the new $v'_{pli}$ value is used to calculate $P_N$ again using Eq. 12 and the comparison between $P_N$ and $P_{Ni}$ is performed for a second time. This whole process is repeated until the difference between $P_N$ and $P_{Ni}$ is less than ±0.1% and at that condition the crack size $a_i$ is in its

final form. For each subsequent load-displacement pair[3], same treatment is applied with the $a_{i+1}$ value inheriting the $a_i$ value from the previous step. Once the crack size adjustment process is complete, the finalized $a_i$ and load-displacement pairs with the original $v'_{pli} \geq 0.002$ are used to evaluate the J-integral using Eq. 3. Combining the J-integral value with $a_i$ yields the J-R curve for the normalization method.

*J-R Curve Determination by the DCPD Technique*

The DCPD technique derives experimental real-time crack sizes based on the potential drop measurement across an area in the specimen. Similar to the normalization method, the J-integral calculation in the DCPD technique is same as in the UC method. Combining the J-integral calculation with crack sizes, the J-R curve can be determined from the DCPD technique.

A number of constitutive equations exist for converting the potential drop measurement into the crack size in the DCPD technique. Among those constitutive equations, Johnson's equation [15, 16] has been widely used and is given by:

$$a = \frac{2W}{\pi}\cos^{-1}\frac{\cosh(\pi y / 2W)}{\cosh\{(U/U_0)\cosh^{-1}[\cosh(\pi y/2W)/\cos(\pi a_0/2W)]\}} \qquad (14)$$

where a is the crack length corresponding to potential drop U, y is one half of the potential gage span (i.e. 0.05 inch per Fig. 4(b)), and $a_0$ and $U_0$ are initial crack length and potential drop, respectively. Based on the crack size calculation in Eq. 14 and the corresponding J-integral calculation in Eq. 3, the original DCPD J-R curve is determined with one example shown in Fig. 6.

The initial portion of the J-R curve in Fig. 6 indicates fast crack growth and does not follow the blunting line closely, resulting in a relatively low $J_q$ value. Indeed, as noted in the

[3] The subsequent load-displacement pairs include all the load-displacement data after the first load-displacement pair with the original $v'_{pli} \geq 0.002$.

work of Bakker [17], during the J-R curve test material potential drop can also result from deformation, crack blunting, and void growth in the process zone ahead of the crack. If the influences of these factors are not accounted in the crack length prediction, the DCPD technique would not predict the crack size accurately and can result in much lower $J_q$ values. Therefore adjustment on original DCPD J-R curve is needed. In early DCPD adjustment methods [18], a slope change point, counted as the critical point distinguishing crack blunting from the onset of slow stable crack growth, is identified by visual inspection of the displacement-potential drop curve. However the slope change point in displacement-potential drop curve of a test may not be clearly identified on occasion and the selection of the critical point tends to be arbitrary, so the repeatability of the analysis is poor. In a more recent work by Chen et al. [19], new DCPD adjustment methods were developed with improved repeatability and excellent match with the UC and normalization methods in terms of $J_q$ values. The major drawback in that method is that the post-adjustment DCPD tearing modulus results show an average difference of 17% from the UC and normalization results. A possible explanation for that result is that since the potential gage span in that work was relatively large, the potential drop signal was measured from a large volume of material which enhanced the influence of plastic deformation on the DCPD measurement.

In order to address these issues, shorter potential gage span is adopted in this study. In addition, a newly-developed semi-empirical DCPD adjustment procedure is proposed. The DCPD adjustment procedure is mainly composed of two steps. The first step aims for identifying the critical point distinguishing crack blunting from the onset of slow stable crack growth. To achieve this, first order derivative of the original DCPD J-R curve coupled with Savitzky-Golay [20] second order polynomial smoothing with 19 points of window is applied as shown in Fig.

7(a). The peak point in Fig. 7(a) represents the data point from which the slope of the original DCPD J-R curve starts to decrease and is indicative of the onset of slow stable crack growth. Therefore the peak point is selected as the critical point. The combination of first order derivative of the original DCPD J-R curve and Savitzky-Golay smoothing eliminates the ambiguity in the selection of the critical point and greatly suppress the noise, if there is any, in the original DCPD J-R curve data for the critical point selection. Once the critical point is identified, all data points prior to and including the critical point itself from the original DCPD J-R curve are shifted left on the blunting line (Fig. 7(b)), which completes the first step of the DCPD adjustment procedure. The second step of the DCPD adjustment procedure is to adjust the crack size for data points subsequent to the critical point in the original DCPD J-R curve so that the final crack extension prediction from the DCPD technique matches the measured final crack extension (Fig. 7(b)). To do so, the crack size of the ith data point subsequent to the critical point in the original DCPD J-R curve is adjusted according to the following equation [17]:

$$a_{pdi'} = \Delta a_{pdcritical'} + \Delta a_{pdi} - \Delta a_{pdcritical} - \frac{u_{pdi} - u_{pdcritical}}{u_{pdfinal} - u_{pdcritical}} (\Delta a_{pdfinal} - \Delta a_{pdcritical} - \Delta a') \quad (15)$$

where $\Delta a_{pdcritical'}$ is the crack extension of the critical point after the first step adjustment, $\Delta a_{pdi}$ is the original DCPD crack extension for the ith data point, $\Delta a_{pdcritical}$ is the original crack extension of the critical point, $u_{pdi}$ is the displacement record for the ith data point, $u_{pdcritical}$ is the displacement record for the critical point, $u_{pdfinal}$ is the displacement record for the last data point in the J-R curve, $\Delta a_{pdfinal}$ is the original DCPD crack extension for the last data point in the J-R curve, and $\Delta a'$ is defined by:

$$\Delta a' = \Delta a_{measured} - \Delta a_{pdcritical'} \quad (16)$$

where $\Delta a_{measured}$ is the optically measured final crack extension. Once the updated crack sizes from the DCPD adjustment procedure become available, they are used to recalculate J-integral values.

*Comparison of J-R Curves Determined by the UC Method, the Normalization Method, and the DCPD Technique after Adjustment*

Major J-R curve test results, namely $J_q$ value and the J-R curve slope for tearing modulus determination, are summarized in Table 2. Excellent agreement is observed between J-R curves from the normalization method and adjusted DCPD J-R curves in all tests. The average differences for $J_q$ and J-R curve slopes between the normalization method and the DCPD technique after adjustment are only about 3.3% and 9.5%, respectively. Indeed, J-R curves from the normalization method and the DCPD technique after adjustment essentially match each other as shown in Fig. 8(a)&(b). For J-R curve results based on the UC method, Table 2 reveals substantial deviation in $J_q$ values between the UC method and the normalization or DCPD method, except for specimen 4-LT and 5-LT. Fig. 8(a) further confirms the apparent difference in J-R curves between the UC method and the normalization or DCPD method. A closer look of J-R curve results from the UC method indicates underprediction of the crack extension by the UC method as shown in Fig. 9. Underprediction of the crack extension would result in high J-integral value in the J-integral calculation if load and displacement data are same. In addition, this also shifts the J-R curve to the left and further increases the $J_q$ value. Only if the UC method underpredicts the crack extension by a very small value, which is the case for specimen 4-LT and 5-LT as shown in Fig. 9, the J-R curve from the UC method can be similar to those from the normalization or DCPD method as in Fig. 8(b).

## Conclusions

J-R curve testing was performed at 24°C and 500°C on standard 0.18T DC(T) specimens made from type 316L stainless steel in both T-L and L-T orientations. In order to address the issue associated with the J-R curve determination with the UC method, especially at elevated temperatures and small specimen testing, alternative J-R curve analysis methods, namely the normalization method and the DCPD technique, were investigated in this study. The normalization method was able to yield valid J-R curves in all tests. The J-R curves from the DCPD technique need adjustment to account for the potential drop induced by plastic deformation, crack blunting, etc. and after applying a newly-developed DCPD adjustment procedure, the post-adjusted DCPD J-R curves essentially matched J-R curves from the normalization method. In contrast, the UC method underpredicted the crack extension in all tests resulting in substantial deviation in the derived J-R curves manifested by higher $J_q$ values than the normalization or DCPD method. Only for tests where the UC method underpredicted the crack extension by a very small value, J-R curves determined by the UC method were similar to those determined by the normalization or DCPD method.

## Acknowledgement

The authors would like to extend their appreciation to Eric Manneschmidt for performing part of mechanical testing, and to Dr. Lizhen Tan for technical review.

**References**

1. Zhu, X.K. Lam, P.S. and Chao, Y.J., "Application of Normalization Method to Fracture Resistance Testing for Storage Tank A285 Carbon Steel," *Int. J. Pres. Ves. Pip.*, Vol. 86, 2009, pp. 669-676.

2. Kim, S.W. Tanigawa, H. Hirose, T. and Kohyama, A., "Effects of Surface Morphology and Distributed Inclusions on the Low Cycle Fatigue Behavior of Miniaturized Specimens of F82H Steel," *Small Specimen Test Techniques: 5th Volume, ASTM STP 1502*, M. Sokolov, Eds., ASTM International, West Conshohocken, PA, 2009, p. 159.

3. ASTM E1820-11: Standard Test Method for Measurement of Fracture Toughness, *Annual Book of ASTM Standards*, ASTM International, West Conshohocken, PA, 2011.

4. Herrera, R. and Landes, J.D., "Direct J-R Curve Analysis: A Guide to the Methodology," *Fracture Mechanics: Twenty-First Symposium, ASTM STP 1074*, J. Gudas, J. Joyce, and E. Hackett, Eds., ASTM International, West Conshohocken, PA, 1990, p. 24.

5. Landes, J. Zhou, Z. Lee, K. and Herrera, R., "Normalization Method for Developing J-R Curves with the Lmn Function," *J. Test. Eval.*, Vol. 19, 1991, pp. 305-311.

6. Joyce, J., "Analysis of a High Rate Round Robin Based on Proposed Annexes to ASTM E 1820," *J. Test. Eval.*, Vol. 29, 2001, pp. 329-351.

7. Lee, K., "Elastic-Plastic Fracture Toughness Determination under Some Difficult Conditions," PhD Dissertation, University of Tennessee, Knoxville, 1995.

8. Hicks, M.A. and Pickard, A.C., "A Comparison of Theoretical and Experimental Methods of Calibrating the Electrical Potential Drop Technique for Crack Length Determination," *Int. J. Fract.*, Vol. 20, 1982, pp. 91-101.

9. Lowes, J.M. and Featnehough, G.D., "The Detection of Slow Crack Growth in Crack Opening Displacement Specimens using an Electrical Potential Method," *Eng. Fract. Mech.,* Vol. 3, 1971, pp. 103-104.

10. McGowan, J.J. and Nanstad, R.K., "Direct Comparison of Unloading Compliance and Potential Drop Techniques in J-integral Testing," *SEM Fall Conference, Computer-Aided Testing and Modal Analysis,* Milwaukee, WI, Nov. 4-7, 1984.

11. Ritchie, R.O. and Bathe, K.J., "On the Calibration of the Electrical Potential Technique for Monitoring Crack Growth using Finite Element Methods," *Int. J. Fract.,* Vol. 15, 1979, pp. 47-55.

12. Tong, J., "Notes on Direct Current Potential Drop Calibration for Crack Growth in Compact Tension Specimens," *J. Test. Eval.,* Vol. 29, 2001, pp. 402-406.

13. ASTM E647-11, Standard Test Method for Measurement of Fatigue Crack Growth Rates, *Annual Book of ASTM Standards,* ASTM International, West Conshohocken, PA, 2011.

14. Turner, C. E., "The Eta Factor," *Post Yield Fracture Mechanics, Second Ed.,* Elsevier Applied Science Publishers, London and New York, 1984, p. 451.

15. Johnson, H.H., "Calibrating the Electrical Potential Method for Studying Slow Crack Growth," *Mater. Res. Stand.,* Vol. 5, 1965, pp. 442-445.

16. Schwalbe, K.H. and Hellmann, D., "Application of the Electrical Potential Method to Crack Length Measurements using Johnson Formula," *J. Test. Eval.,* Vol. 9, 1981, pp. 218-220.

17. Bakker, A.D., "A DC Potential Drop Procedure for Crack Initiation and R-Curve Measurements During Ductile Fracture Tests," *Elastic-Plastic Fracture Test Methods: The User's Experience, ASTM STP 856,* F. Loss, and E. Wessel, Eds., ASTM International, West Conshohocken, PA, 1985, p. 394.

18. Dufresne, J. Henry, B. and Larsson, H., “Fracture Toughness of Irradiated AISI 304 and 316L Stainless Steels,” *Effects of Radiation on Structural Materials, ASTM STP 683*, J. Sprague, and D. Kramer, Eds., ASTM International, West Conshohocken, PA, 1979, p. 511.

19. Chen, X. Nanstad, R.K. and Sokolov, M.A., “Application of Direct Current Potential Drop for Fracture Toughness Measurement,” *22nd International Conference on Structural Mechanics in Reactor Technology*, San Francisco, CA, Aug. 18-23, 2013.

20. Savitzky, A. and Golay, M., "Smoothing + Differentiation of Data by Simplified Least Squares Procedures," *Anal. Chem.*, Vol. 36, 1964, pp. 1627-1639.

**Tables**

Table 1 Material constants at testing temperatures

| Material | Temperature (°C) | Yield Strength (MPa) | Tensile Strength (MPa) | Young's Modulus (GPa) |
|---|---|---|---|---|
| SS316L | 24 | 423.5 | 810.1 | 193.1 |
| | 500 | 131.0 | 413.7 | 165.0 |

Table 2 Comparison of J-R curve results among the UC method, the normalization method, and the DCPD technique after adjustment

| Specimen ID[a] | Temperature (°C) | $J_q$ (KJ/m$^2$) | | | J-R curve slope[b] | | |
|---|---|---|---|---|---|---|---|
| | | UC | Normalization | adjusted DCPD | UC | Normalization | adjusted DCPD |
| 1-TL | 24 | 304.3 | 224.4 | 234.4 | 163.9 | 189.1 | 169.8 |
| 2-TL | 24 | 330.7 | 256.2 | 262.5 | 97.0 | 118.0 | 110.5 |
| 3-TL | 24 | 303.2 | 253.3 | 262.1 | 124.1 | 144.3 | 122.1 |
| 4-LT | 24 | 430.9 | 419.0 | 415.1 | 232.8 | 241.9 | 244.2 |
| 5-LT | 24 | 440.2 | 445.9 | 421.1 | 187.0 | 188.0 | 204.7 |
| 6-TL | 500 | NA | 189.6 | 197.9 | NA | 108.3 | 98.1 |
| 7-TL | 500 | NA | 182.0 | 190.8 | NA | 116.0 | 103.7 |
| 8-LT | 500 | NA | 285.5 | 289.9 | NA | 179.7 | 161.9 |
| 9-LT | 500 | NA | 279.0 | 286.0 | NA | 184.1 | 158.1 |

[a]TL and LT designate the orientation of the specimen
[b]J-R curve slope is determined by linear fitting of the J-R curve portion between the first and second exclusion lines

**List of Figure Captions**

Fig. 1 Comparison of load-displacement records for the unloading compliance method and the normalization method in a J-R curve test

Fig. 2 Schematic for (a) direct current potential drop measurement and (b) crack growth induced increase in potential drop

Fig. 3 Standard 0.18T disk-shaped compact specimen design

Fig. 4 Locations of current and potential probes for direct current potential drop measurement

Fig. 5 Normalization function fit procedures: (a) calculation of normalized load and plastic displacement; (b) determination of eligible data for the normalization function fit based on the tangent line drawn from the final load displacement pair to the remaining data; (c) starting from the normalized plastic displacement of 0.001, application of the normalization function fit on eligible data from (b)

Fig. 6 original J-R curve determined with the DCPD technique

Fig. 7 (a) critical point selection based on the peak point of the first order derivative of the original DCPD J-R curve in Fig. 6 with Savitzky-Golay smoothing; (b) adjustment of the original DCPD J-R curve in Fig. 6

Fig. 8 Comparison of J-R curves from the unloading compliance method, the normalization method, and the DCPD technique after adjustment. (a) and (b) represent two cases showing that the unloading compliance method underpredicted the final crack extension by a large amount and a small amount, respectively

Fig. 9 Comparison of measured final crack extension with the unloading compliance method predicted final crack extension

**Figures**

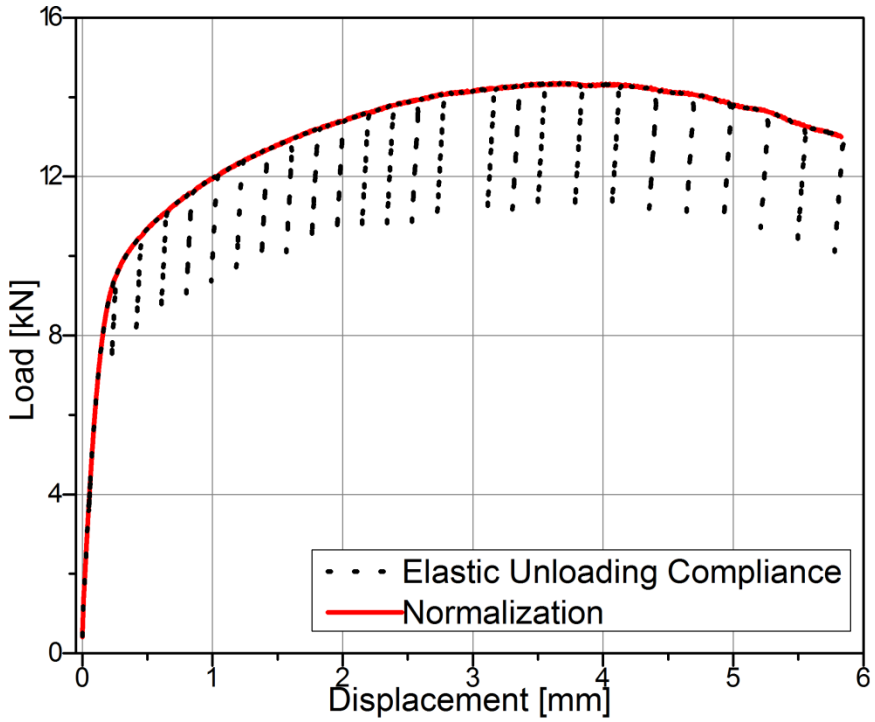


Fig. 1 Comparison of load-displacement records for the unloading compliance method and the normalization method in a J-R curve test

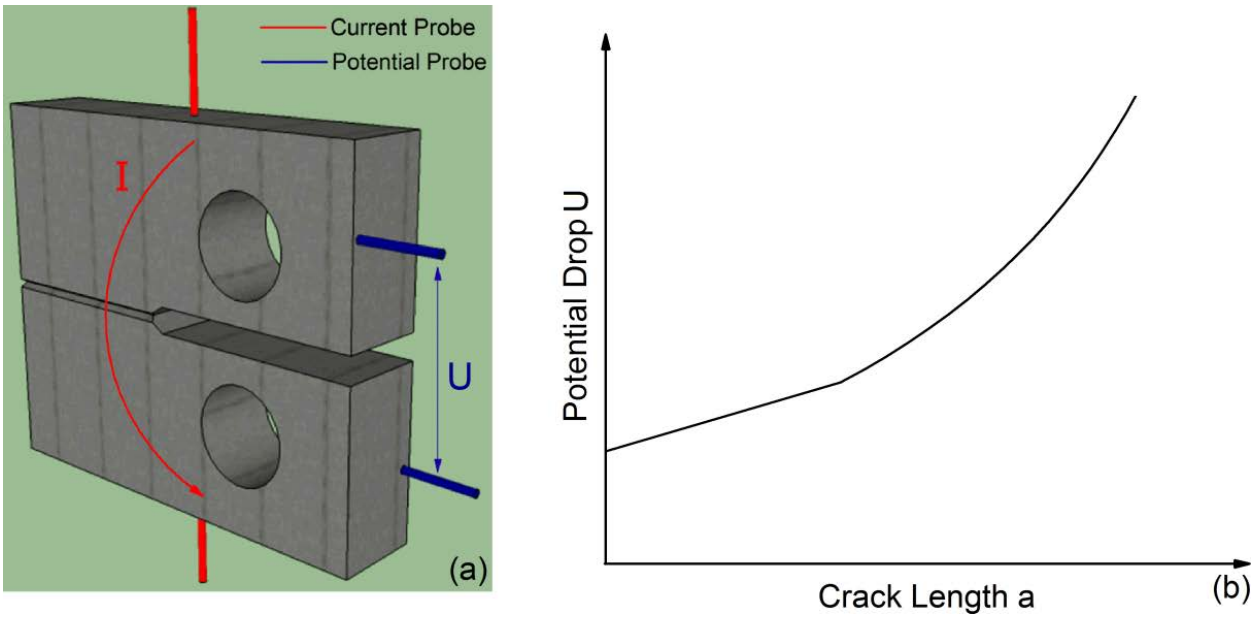


Fig. 2 Schematic for (a) direct current potential drop measurement and (b) crack growth induced increase in potential drop

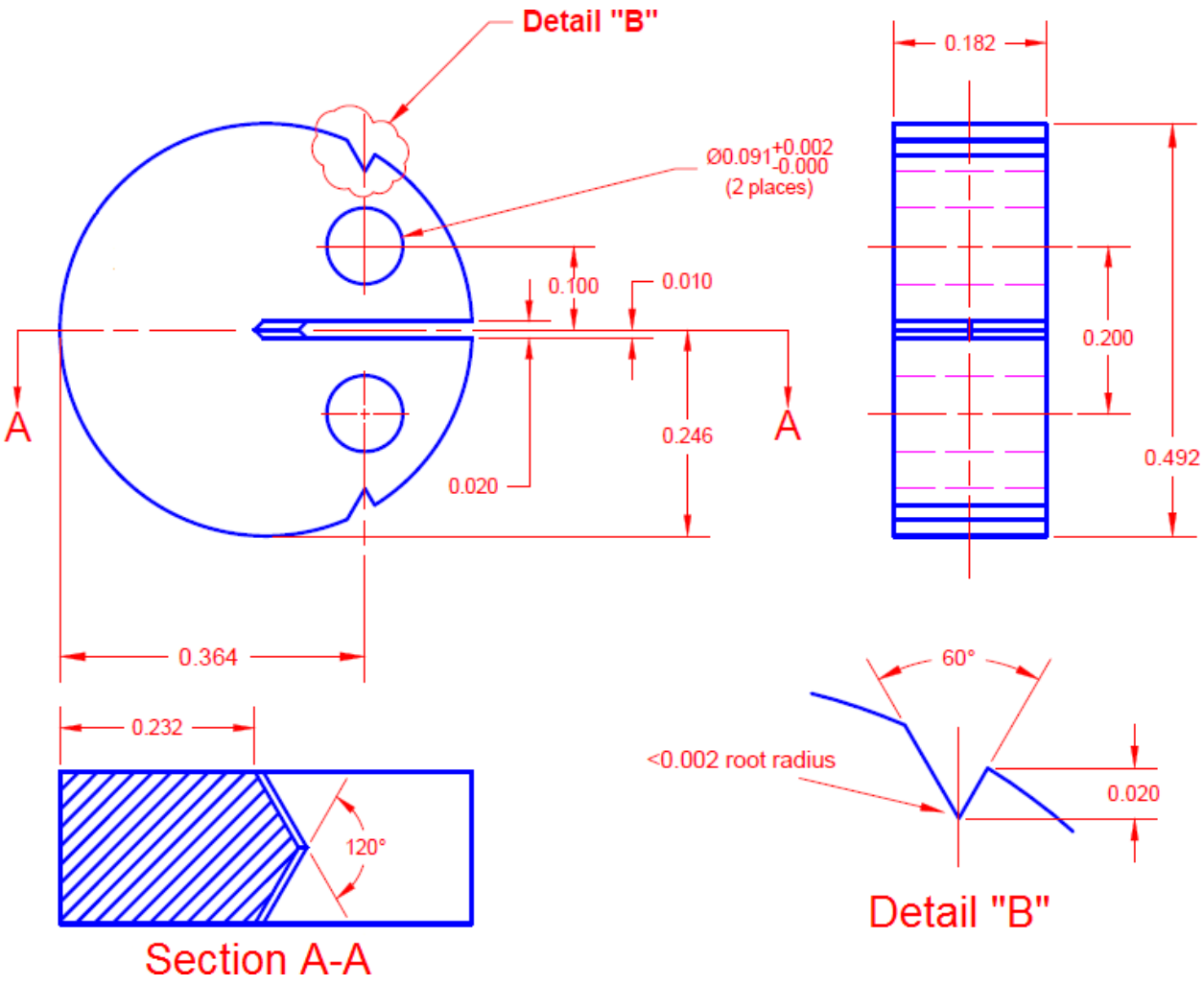


Fig. 3 Standard 0.18T disk-shaped compact specimen design

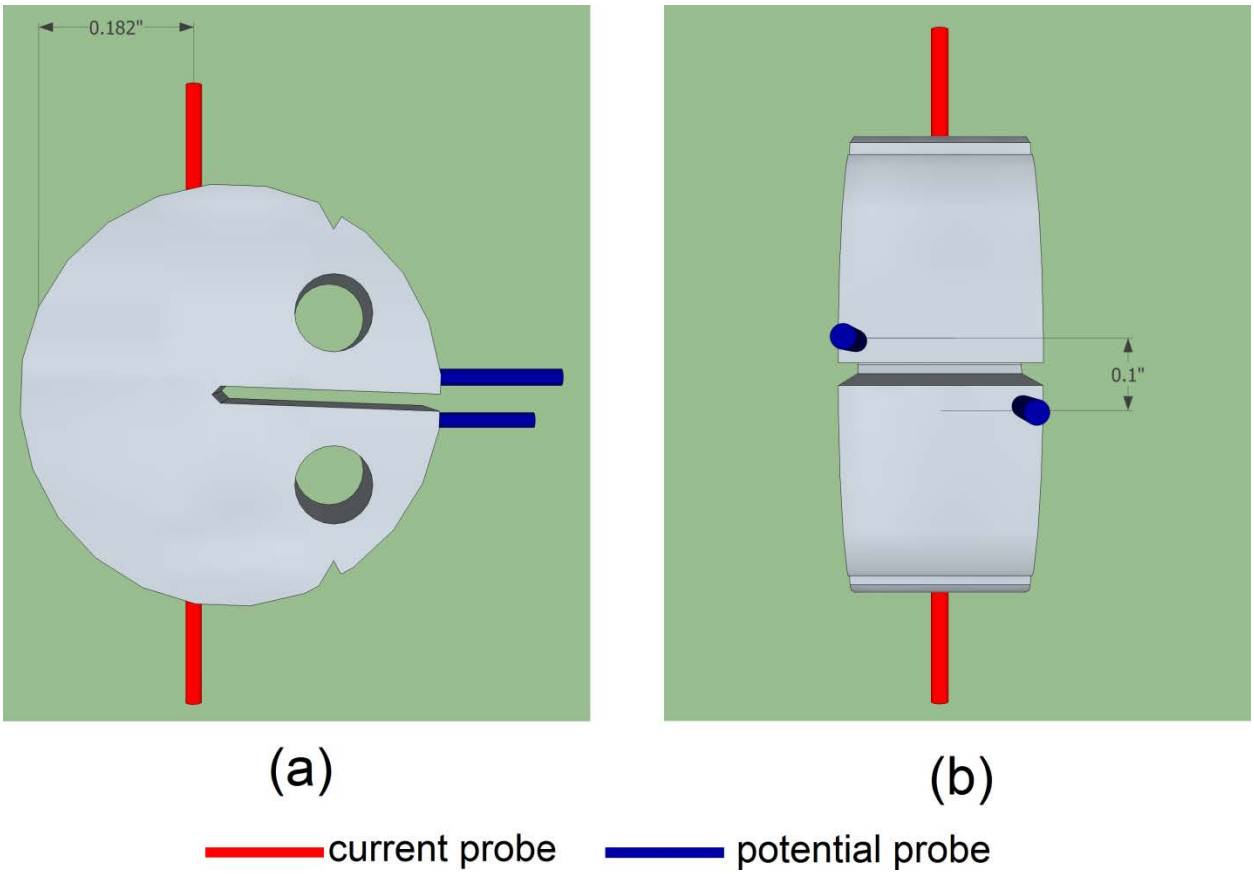


Fig. 4 Locations of current and potential probes for direct current potential drop measurement

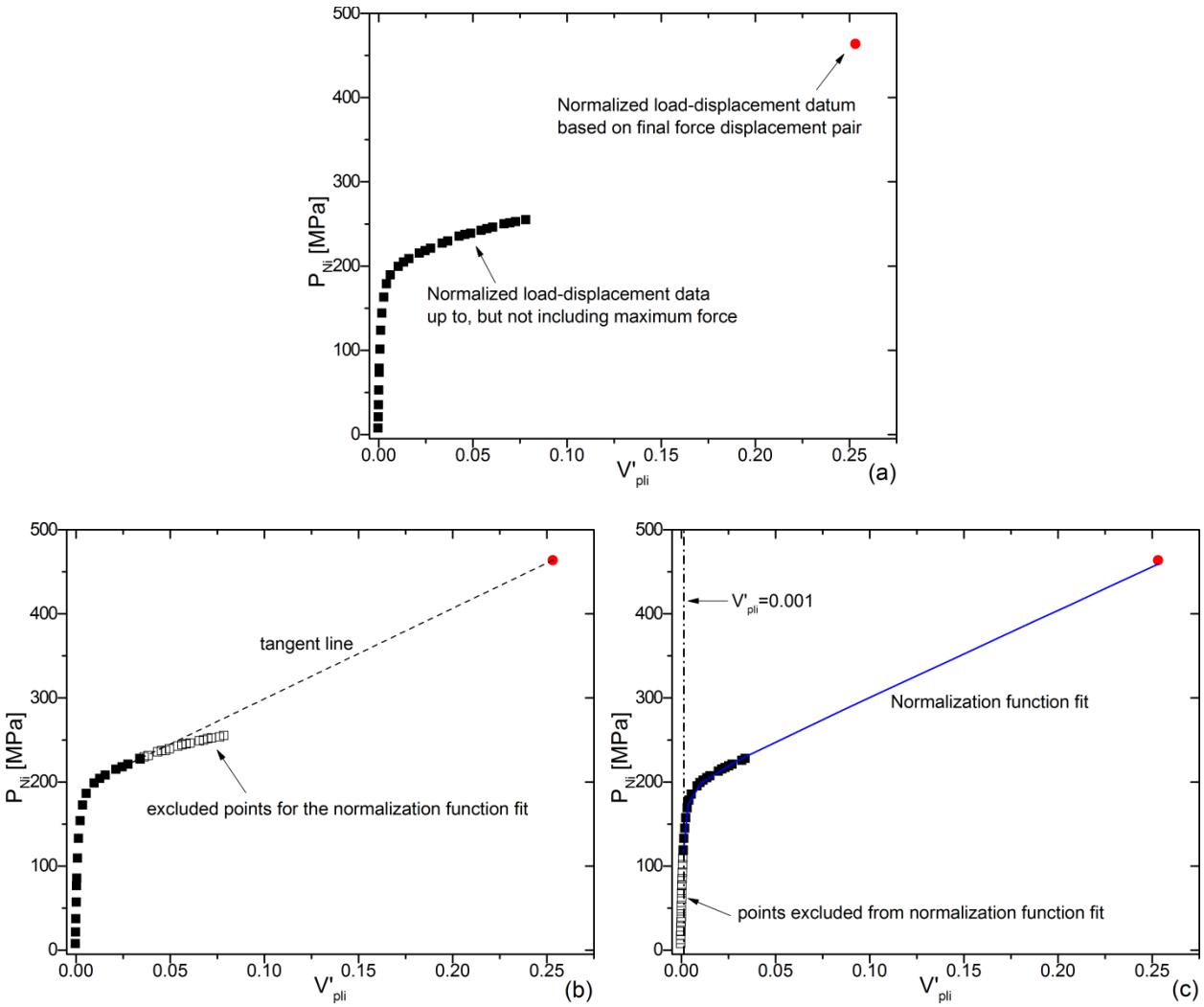


Fig. 5 Normalization function fit procedures: (a) calculation of normalized load and plastic displacement; (b) determination of eligible data for the normalization function fit based on the tangent line drawn from the final load displacement pair to the remaining data; (c) starting from the normalized plastic displacement of 0.001, application of the normalization function fit on eligible data from (b)

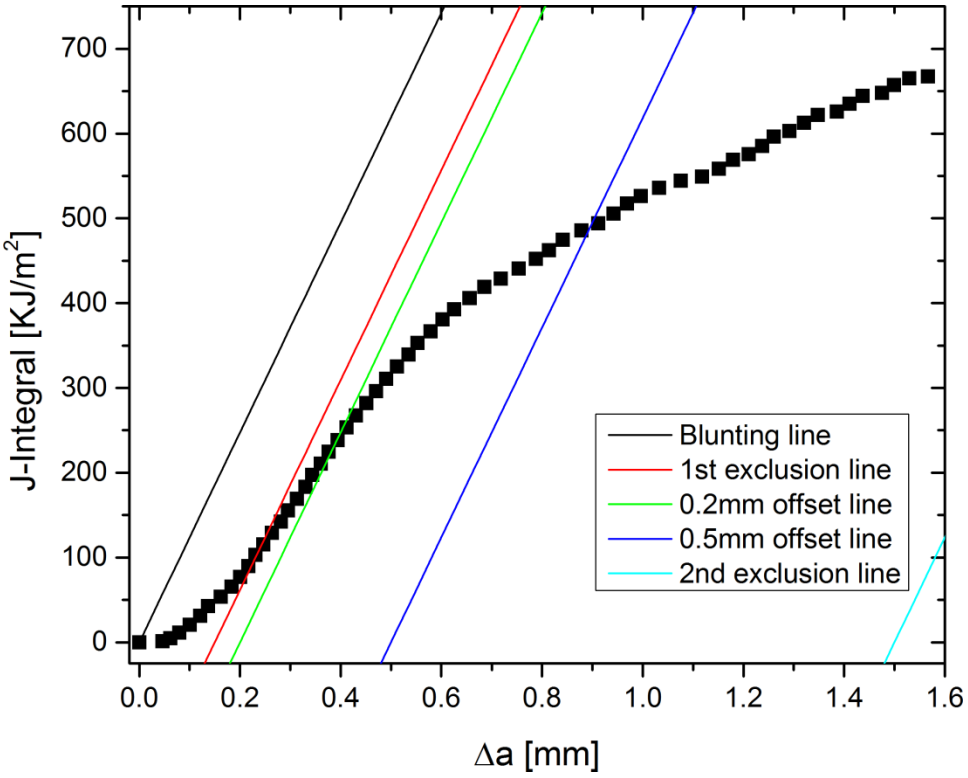


Fig. 6 original J-R curve determined with the DCPD technique

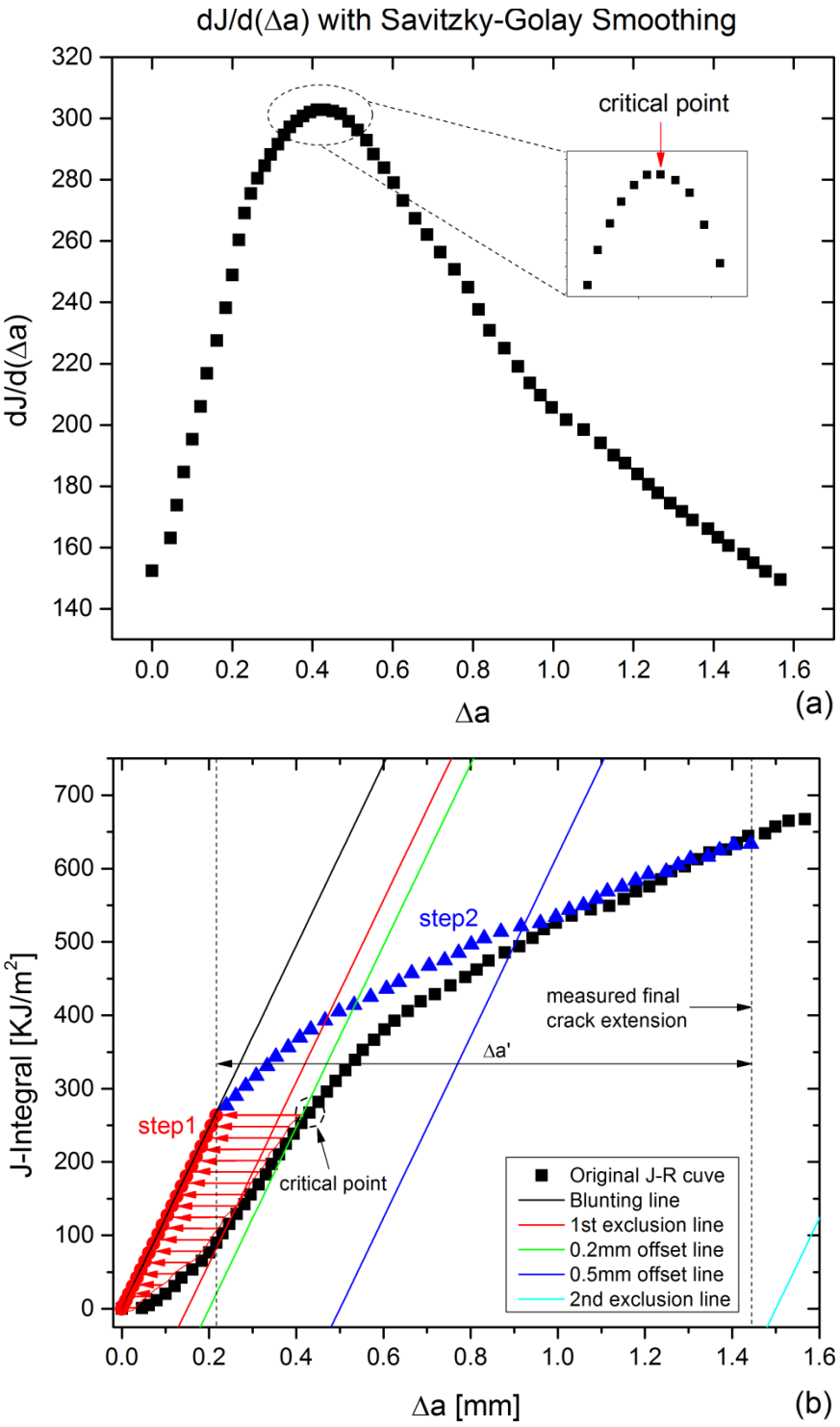


Fig. 7 (a) critical point selection based on the peak point of the first order derivative of the original DCPD J-R curve in Fig. 6 with Savitzky-Golay smoothing; (b) adjustment of the original DCPD J-R curve in Fig. 6

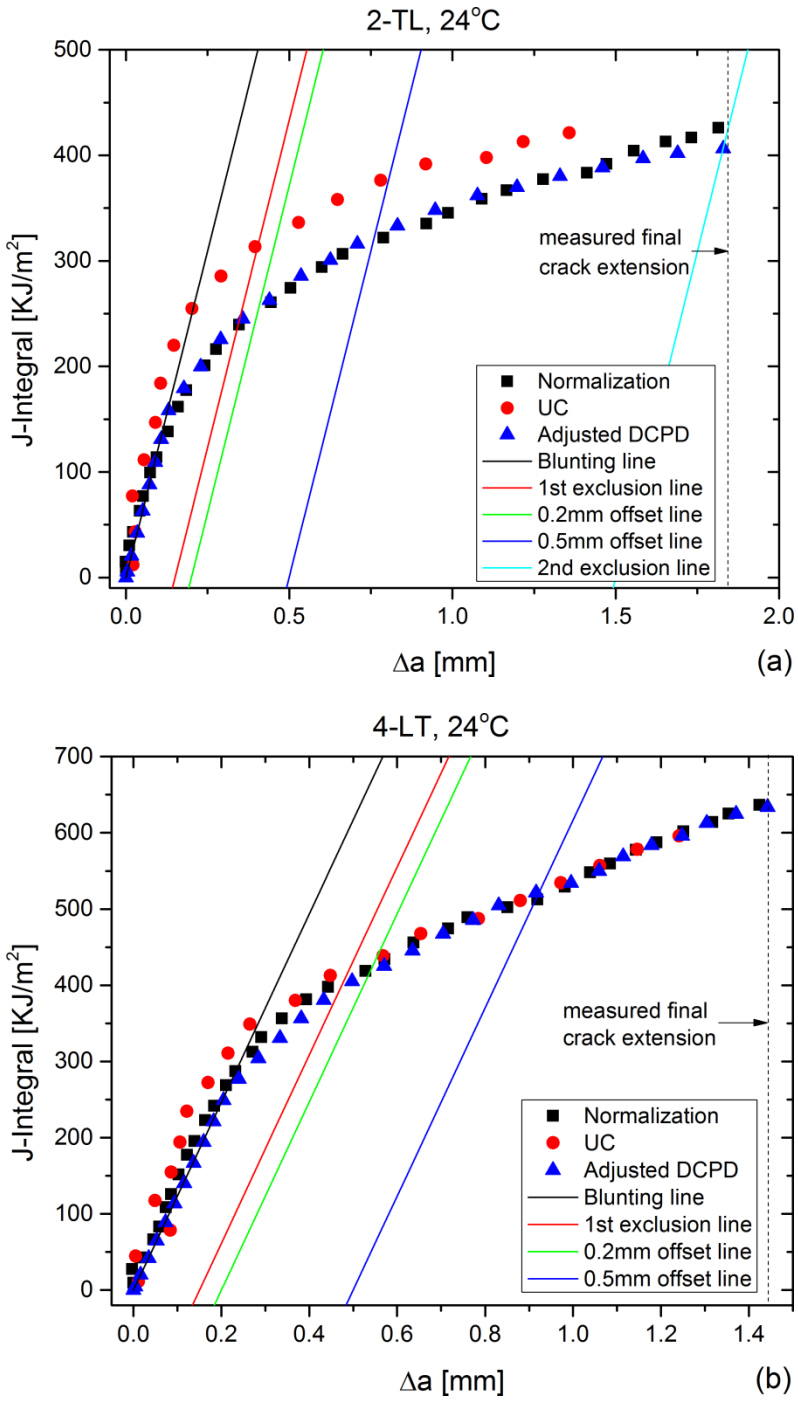


Fig. 8 Comparison of J-R curves from the unloading compliance method, the normalization method, and the DCPD technique after adjustment. (a) and (b) represent two cases showing that the unloading compliance method underpredicted the final crack extension by a large amount and a small amount, respectively

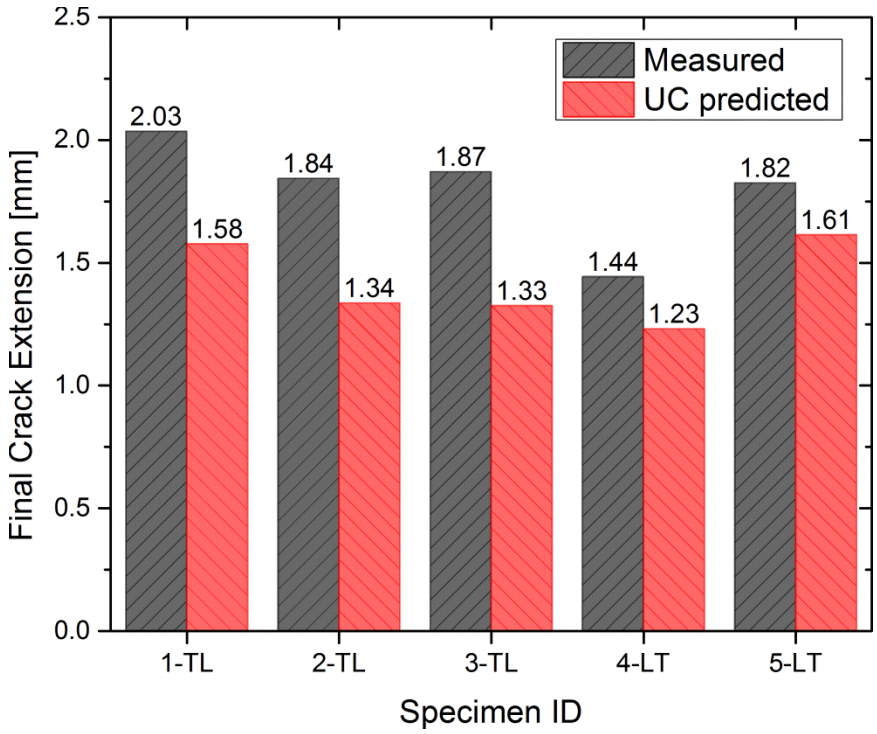


Fig. 9 Comparison of measured final crack extension with the unloading compliance method predicted final crack extension